

## PAIN

# Pharmacological reversal of a pain phenotype in iPSC-derived sensory neurons and patients with inherited erythromelalgia

Lishuang Cao,<sup>1\*</sup> Aoibhinn McDonnell,<sup>1\*</sup> Anja Nitzsche,<sup>1\*</sup> Aristos Alexandrou,<sup>1</sup> Pierre-Philippe Saintot,<sup>1</sup> Alexandre J.C. Loucif,<sup>1</sup> Adam R. Brown,<sup>1</sup> Gareth Young,<sup>1</sup> Malgorzata Mis,<sup>2</sup> Andrew Randall,<sup>3</sup> Stephen G. Waxman,<sup>4</sup> Philip Stanley,<sup>1</sup> Simon Kirby,<sup>1</sup> Sanela Tarabar,<sup>5</sup> Alex Gutteridge,<sup>1</sup> Richard Butt,<sup>1</sup> Ruth M. McKernan,<sup>1</sup> Paul Whiting,<sup>1</sup> Zahid Ali,<sup>1†</sup> James Bilsland,<sup>1†‡</sup> Edward B. Stevens<sup>1†‡</sup>

In common with other chronic pain conditions, there is an unmet clinical need in the treatment of inherited erythromelalgia (IEM). The *SCN9A* gene encoding the sodium channel Nav1.7 expressed in the peripheral nervous system plays a critical role in IEM. A gain-of-function mutation in this sodium channel leads to aberrant sensory neuronal activity and extreme pain, particularly in response to heat. Five patients with IEM were treated with a new potent and selective compound that blocked the Nav1.7 sodium channel resulting in a decrease in heat-induced pain in most of the patients. We derived induced pluripotent stem cell (iPSC) lines from four of five subjects and produced sensory neurons that emulated the clinical phenotype of hyperexcitability and aberrant responses to heat stimuli. When we compared the severity of the clinical phenotype with the hyperexcitability of the iPSC-derived sensory neurons, we saw a trend toward a correlation for individual mutations. The *in vitro* IEM phenotype was sensitive to Nav1.7 blockers, including the clinical test agent. Given the importance of peripherally expressed sodium channels in many pain conditions, our approach may have broader utility for a wide range of pain and sensory conditions.

## INTRODUCTION

Individual *SCN9A* mutations leading to a loss of channel function have been associated with congenital insensitivity to pain, whereas gain-of-function mutations in the *SCN9A* gene have been associated with chronic painful conditions including inherited erythromelalgia (IEM), paroxysmal extreme pain disorder, and idiopathic small fiber neuropathy. IEM is a chronic, extreme pain condition that results in burning pain sensations and erythema, particularly in the distal extremities (1–4). The pain is often episodic and mild heat or a body temperature increase is a common major trigger for attacks of pain in IEM (4).

The development of selective Nav1.7 blockers, in common with other new analgesic drug targets, has been hampered by the lack of robust preclinical to clinical translation. In particular, a complete understanding of the role of Nav1.7 in action potential firing in human sensory neurons has been limited by the reliance of electrophysiological studies on heterologous expression of the channel. For example, all reported IEM Nav1.7 mutations are associated with a hyperpolarized voltage dependence of activation and/or voltage dependence of fast inactivation after heterologous expression in mammalian cell lines (5–11). However, the absolute value and magnitude of changes in gating parameters for individual IEM mutations vary between different laboratories and may not directly translate to native Nav1.7 in human sensory neurons (5, 6, 10).

Overexpression of IEM Nav1.7 mutations in mouse dorsal root ganglion neurons has been used to understand the contribution of the

changes in channel gating to action potential firing properties (12). The interpretation is, however, compromised by the expression level of human Nav1.7 relative to rodent tetrodotoxin-sensitive sodium channels and appropriate processing and assembly of the human isoform in a rodent neuronal background. Human pluripotent stem cell (PSC)-derived sensory neurons (13, 14) provide an improved physiologically relevant model to investigate the relationship between a human ion channel in its native environment and neuronal excitability.

Induced PSC (iPSC) technology allows generation of cells from patients, which retain the genetic identity of the donor and can recapitulate disease pathology in differentiated progeny. This has the potential to enable new therapeutics to be tested on both individual patients and their cognate iPSC-derived cells to further understand both clinical efficacy and effects on the underlying cellular phenotype. However, to date, it is unclear to what extent the response of a therapeutic agent in an iPSC disease model translates to the clinic.

Here, we investigated the effect of a new selective Nav1.7 blocker, PF-05089771, on the inhibition of heat-evoked pain in five IEM human subjects carrying four different *SCN9A* mutations. Simultaneously, we generated iPSC-derived sensory neurons (iPSC-SNs) from four of five IEM subjects to characterize the neuronal phenotype associated with individual mutations and the effects of selectively blocking Nav1.7 channels on action potential generation.

## RESULTS

### Differentiating iPSCs from IEM patients into functional sensory neurons

Five IEM subjects (three males and two females; average age of 40.2 years) (Table 1) provided informed consent to participate in a double-blind, placebo-controlled clinical study. Extensive clinical phenotyping had previously been performed in these subjects (4). Four of five subjects additionally consented to donate blood for iPSC generation (Table 1).

<sup>1</sup>Pfizer Neuroscience and Pain Research Unit, The Portway Building, Granta Park, Cambridge CB21 6GS, UK. <sup>2</sup>University of Bristol, School of Physiology, Pharmacology, and Neuroscience, Bristol BS8 1TD, UK. <sup>3</sup>Hatherly College of Life and Environmental Sciences, University of Exeter, Prince of Wales Road, Exeter EX4 4PS, UK. <sup>4</sup>Yale Center for Neuroscience and Regeneration Research, Veterans Affairs Medical Center, 950 Campbell Avenue, Building 34, West Haven, CT 06516, USA. <sup>5</sup>Pfizer, 1 Howe Street, New Haven, CT 06511, USA.

\*These authors contributed equally to this work.

†These authors contributed equally to this work.

‡Corresponding author. E-mail: j.bilsland@ucl.ac.uk (J.B.); edward.stevens@pfizer.com (E.B.S.)

**Table 1. Clinical phenotype of IEM subjects.**

Subject ID	SCN9A mutation	Gender	Age at onset of IEM (year)	Pain attack trigger	Consent* to donate blood for iPSC
EM1	S241T	F	17	Heat, exercise	Yes
EM2	I848T	M	4	Heat, exercise	Yes
EM3	V400M	M	>10	Heat, exercise, standing	Yes
EM4	V400M	M	4	Heat, exercise	No
EM5	F1449V	F	<2	Heat, exercise, standing	Yes

\*Consent to donate blood for iPSC generation was optional for subjects in the clinical study.

Peripheral blood mononuclear cells were extracted from donated blood samples. The erythroid progenitor populations of the peripheral blood cells were reprogrammed into iPSCs, and up to three clonal iPSC lines per subject were established. Individual heterozygous mutations in the iPSCs were confirmed through Sanger sequencing (Fig. 1A). We also generated iPSCs from four independent non-IEM donors who were used as a control group in which no mutations in *Nav1.7* associated with paroxysmal extreme pain disorder, IEM, or congenital insensitivity to pain were identified. All iPSC clonal cell lines showed typical morphology for pluripotent cell colonies and expressed the pluripotency marker *Oct4* (Fig. 1B). Array comparative genomic hybridization (CGH) analysis revealed a normal karyotype and comparable number or size of copy number variants between non-IEM donor and IEM subject iPSCs for most iPSC clones (fig. S1, A and B).

We differentiated iPSCs into sensory neurons using a small molecule-based protocol as described previously (13, 14). One week after addition of neural growth factors, the differentiated cells exhibited a neuronal morphology and stained positive for the sensory neuron markers *Brn3a*, *Islet1*, and *peripherin*, with no obvious morphological difference between donor- and study subject-derived neurons (Fig. 1C). Neurons were further matured for another 8 weeks before electrophysiological recordings were obtained. The sensory neurons derived from non-IEM and IEM clonal iPSC lines all expressed *SCN9A* and other sodium channel subtypes as determined by quantitative polymerase chain reaction (qPCR) (fig. S1C). To characterize the functional role of the *Nav1.7* channel in iPSC-SNs using a whole-cell patch-clamp technique, two selective *Nav1.7* blockers were exploited: the clinical compound PF-05089771 and an in vitro tool PF-05153462 (fig. S2, A to C). In comparison to the slow kinetics of inhibition for PF-05089771, PF-05153462 displayed fast rates of blockade and was fully reversible within 10 min, enabling multiple concentrations to be applied to each cell and therefore allowing a more extensive and robust investigation of the contribution of *Nav1.7* to sensory neuron excitability.

Application of PF-05153462 reversibly inhibited the peak sodium current of iPSC-SNs, confirming the functional expression of *Nav1.7*. Comparison of the *Nav1.7* current densities (as defined using inhibition by 100 nM PF-05153462) across iPSC-SN clones revealed no significant differences between the individual clones or between the IEM and non-IEM groups [example traces, Fig. 1D; quantification, Fig. 1E; nonparametric analysis of variance (ANOVA),  $P > 0.05$ ]. In addition, there was no significant difference in the percentage of total sodium current (fig. S3A; nonparametric ANOVA,  $P > 0.05$ ) or current carried by *Nav1.7* (fig. S3B; nonparametric ANOVA,  $P > 0.05$ ) across iPSC-SN clones. These data suggested robust and equivalent expression of *Nav1.7* channels in iPSC-SNs, irrespective of the donor from which they were generated.

### **iPSC-SNs derived from IEM subjects show elevated excitability**

We observed spontaneous action potential firing from a subpopulation of iPSC-SNs at resting membrane potential (Fig. 2A, right). On average, the iPSC-SNs from IEM donors showed a significantly higher proportion of spontaneously firing cells compared to those from non-IEM donors ( $P < 0.05$ , linear logistic model), suggesting higher excitability (Fig. 2B).

Notwithstanding this, iPSC-SNs from subject EM1 (with the S241T mutation) and non-IEM donor D1 showed similar degrees of spontaneous firing, which was only moderately enhanced compared to the other non-IEM donors, suggesting some intrinsic heterogeneity among the iPSC-SNs from both the IEM and non-IEM donors (Fig. 2B). There was a small but statistically significant depolarization of resting membrane potential in the IEM subject cells ( $-57.4 \pm 0.4$  mV;  $n = 272$  with all IEM subjects pooled together) compared to non-IEM donor cells ( $-60 \pm 0.4$  mV;  $n = 158$  for all non-IEM subjects) (fig. S3C;  $P < 0.05$ , ANOVA), which could have contributed to the observed increase in spontaneous activity.

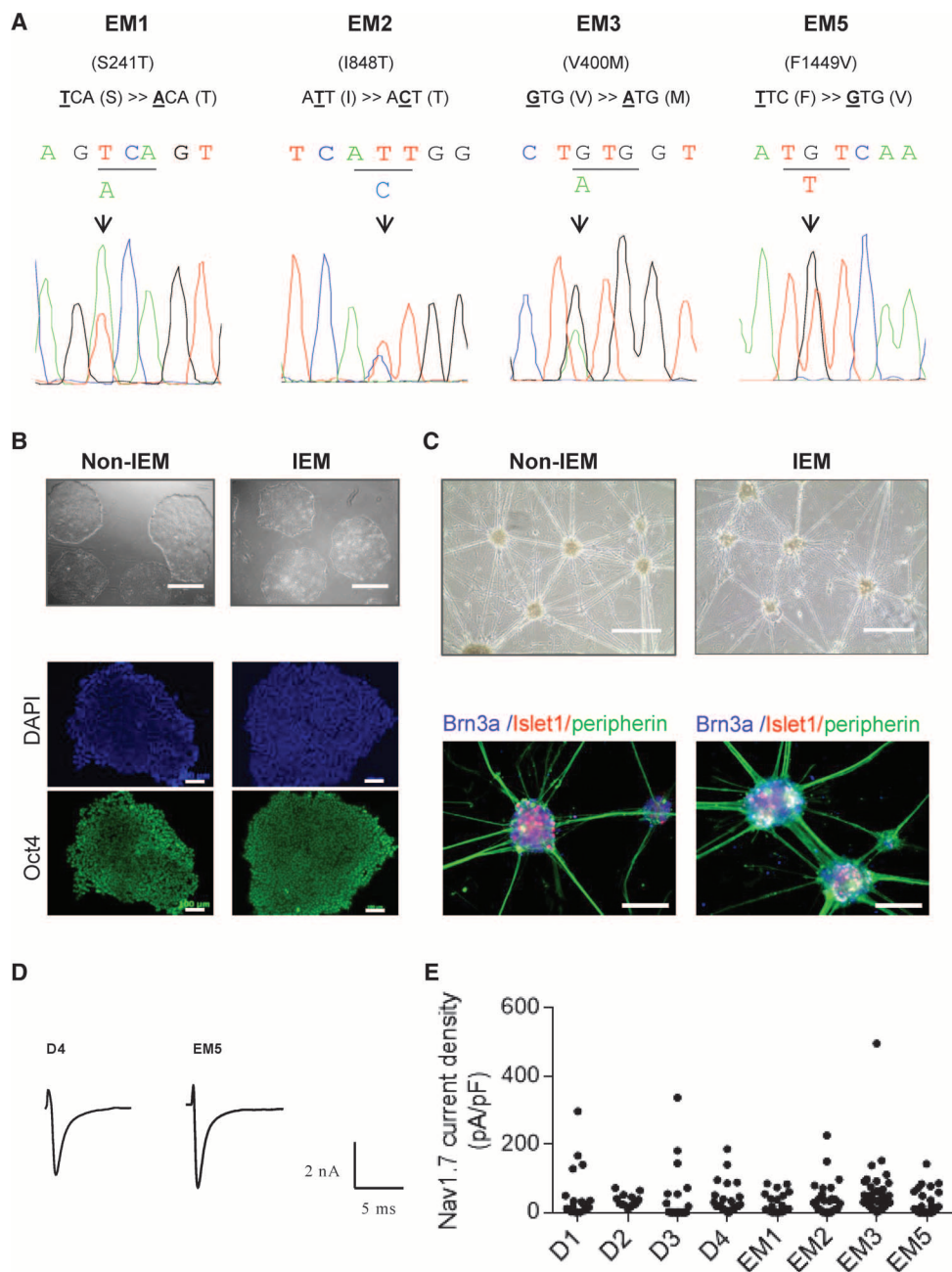
Next, we studied rheobase, the minimal current injection required to evoke an action potential, as a measure of subthreshold contributions to excitability (Fig. 2C). On average, the rheobase was lower in the iPSC-SNs from IEM donors ( $122 \pm 10$  pA;  $n = 270$ ) when compared to neurons from non-IEM donors ( $361 \pm 20$  pA;  $n = 148$ ) (Fig. 2D;  $P < 0.05$ , nonparametric ANOVA). These data suggest that iPSC-SNs from IEM subjects have increased excitability.

We also measured evoked firing frequency in response to increasing amplitude of injected current (Fig. 2E). Although IEM iPSC-SNs gave rise to a higher number of action potentials at low levels of current injection compared to non-IEM cells (Fig. 2F), there was considerable variability in the firing frequency between cells for each iPSC clone; thus, this was not considered a reliable end point for statistical analysis. Therefore, we focused on spontaneous firing and rheobase to determine pharmacological effects of *Nav1.7* blockers.

### **Nav1.7 blockers reduce elevated excitability of IEM iPSC-SNs**

We further tested the effects of the selective *Nav1.7* blocker PF-05153462 on spontaneously firing iPSC-SNs (Fig. 3A). As shown in Fig. 3B, the spontaneous firing of iPSC-SNs from subjects EM2 (I848T mutation) and EM3 (V400M mutation) was reduced by PF-05153462 in a concentration-dependent manner. iPSC-SNs from EM1 (S241T mutation) rarely exhibited spontaneous firing (Fig. 2B); therefore, PF-05153462 was not tested. The spontaneous firing in iPSC-SNs from EM5 (F1449V mutation) was not sustained for sufficient duration to generate a concentration-response curve; therefore, a single concentration of PF-05153462 (100 nM) was tested and found to completely inhibit spontaneous firing

**Fig. 1. iPSCs from IEM subjects and non-IEM donors differentiate into sensory neurons with comparable Nav1.7 activity.** (A) Sanger sequencing of IEM subject-derived iPSCs. The black arrow highlights the heterozygous point mutation in the pherogram. (B) Bright-field images of representative examples of IEM subject-derived and non-IEM donor-derived iPSCs with typical pluripotent-like morphology. Scale bars, 1000  $\mu$ m. Panels below show immunostaining for nuclear Hoechst stain (blue) and expression of the Oct4 pluripotency marker (green). Scale bars, 100  $\mu$ m. DAPI, 4',6-diamidino-2-phenylindole. (C) Bright-field images of representative examples of IEM subject-derived and non-IEM donor-derived iPSCs after differentiation into sensory neurons (iPSC-SNs). Scale bars, 1000  $\mu$ m. Panels below show immunostaining for expression of the sensory neuron marker Brn3a (blue), Islet1 (red), and peripherin (green). Scale bars, 200  $\mu$ m. (D) Example sodium current traces measured in the iPSC-SNs derived from the non-IEM donor (D4) and IEM subject EM5 (carrying the F1449V mutation) showing subtracted currents sensitive to the Nav1.7 blocker. iPSC-SNs were held at  $-110$  mV and stepped to 0 mV to evoke voltage-gated currents, which were partially blocked by 100 nM PF-05153462. (E) Summary of Nav1.7 current density in the non-IEM donor-derived and IEM subject-derived iPSC-SNs. No significant difference was observed among all the clones ( $n = 13$  to 40).



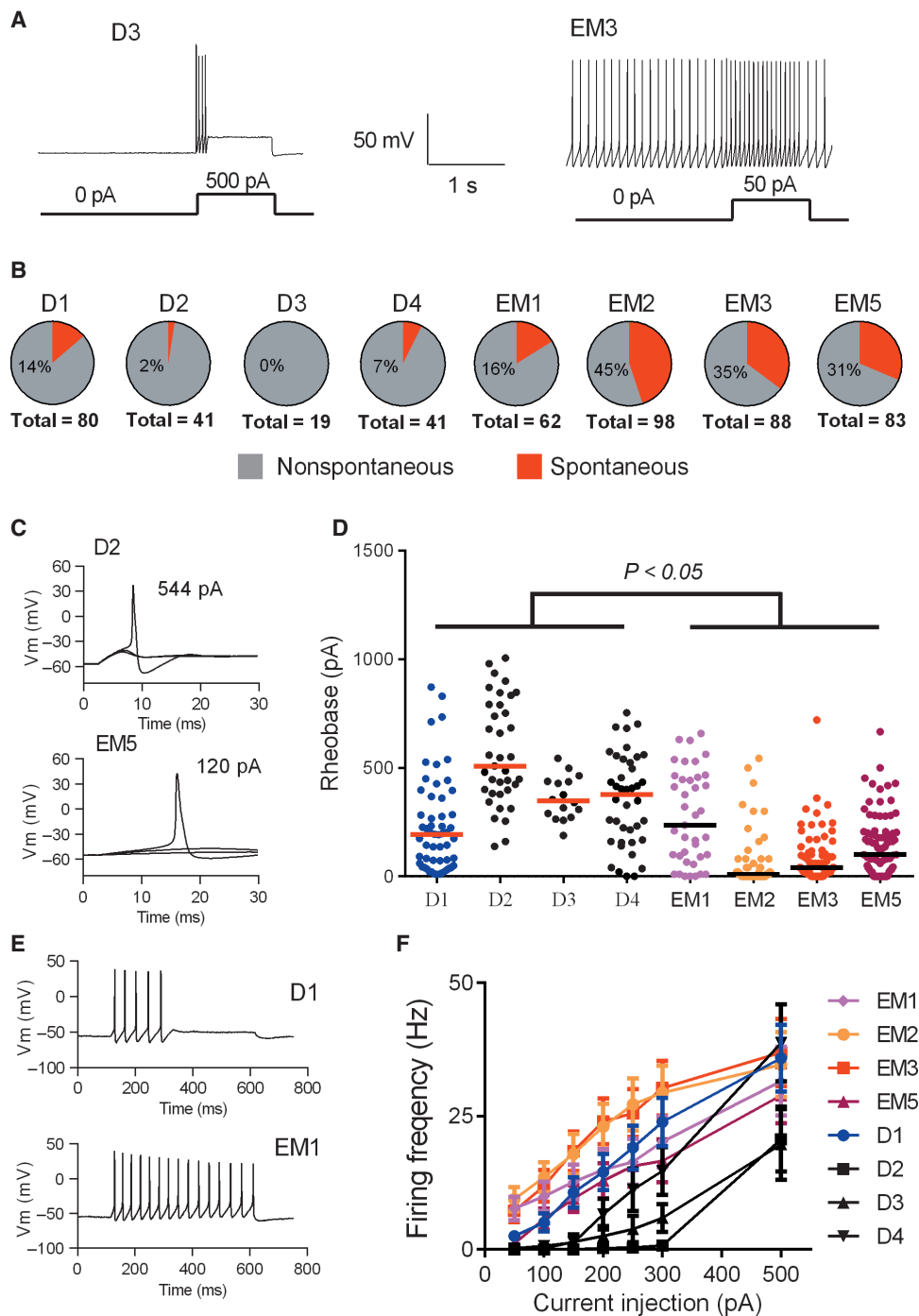
( $n = 5$ ). PF-05089771, the Nav1.7 blocker evaluated in IEM subjects, was also tested on iPSC-SNs from subject EM2, where spontaneous firing was completely blocked at a concentration of 60 nM (Fig. 3C). These data indicate that the gain-of-function mutations present in IEM Nav1.7 channels contribute to the higher incidence of spontaneous firing in iPSC-SNs from IEM subjects.

Next, we investigated the contribution of wild-type and IEM mutant Nav1.7 channels to rheobase of the action potential using PF-05089771 (Fig. 3D). Voltage-clamp recordings of human embryonic kidney 293 cells stably expressing mutant Nav1.7 resulted in similar half-maximal inhibitory concentration ( $IC_{50}$ ) values, ranging from 11 to 36 nM (fig. S2D). Whereas PF-05089771 increased the rheobase in a concentration-

dependent manner for iPSC-SNs from both IEM subjects and non-IEM donors (suggesting a clear role of Nav1.7 in setting threshold), the magnitude of this effect was significantly greater in iPSC-SNs derived from IEM subjects at all three concentrations (Fig. 3E;  $P < 0.05$ , ANOVA;  $n = 6$  to 10 for each concentration). Similar results were obtained from the selective Nav1.7 blocker PF-05153462 at concentrations greater than 10 nM (Fig. 3F;  $P < 0.05$ , ANOVA;  $n = 6$  to 10 for each concentration). The greater contribution of Nav1.7 to rheobase in sensory neurons from IEM subjects compared to non-IEM donors most likely reflects enhanced channel activity as a result of gating shifts associated with the S241T, I848T, V400M, and F1449V mutations. Together, these studies using Nav1.7 blockers strongly suggest that these Nav1.7 gain-of-function

**Fig. 2. Excitability of iPSC-SNs from IEM and non-IEM subjects.**

(A) Representative traces of spontaneous firing in sensory neurons derived from iPSCs from IEM subject EM3 (V400M mutation) and non-IEM control subject D3. (B) Quantification of the number of spontaneous firing iPSC-SNs versus nonspontaneous firing iPSC-SNs from non-IEM and IEM subjects ( $n = 19$  to  $98$ ;  $P < 0.05$ , linear logistic model). (C) Representative current-clamp traces showing subthreshold responses and subsequent action potentials evoked until reaching current thresholds (rheobase) of  $544$  pA for non-IEM subject D3 iPSC-SNs and  $120$  pA for IEM subject EM5 (F1449V mutation) iPSC-SNs. (D) Quantification of action potential rheobase comparing healthy control donor iPSC-SNs and IEM subject iPSC-SNs ( $n = 16$  to  $86$ ;  $P < 0.05$ , nonparametric ANOVA). (E) Representative traces showing train of action potentials evoked in non-IEM control subject D1 and IEM subject EM1 (S241T mutation) iPSC-SNs after inducing depolarization by  $100$ -pA current injection. (F) Quantification of action potential frequency induced by current injection ( $n = 10$  to  $46$ ).



IEM mutations underpin the increased excitability of iPSC-SNs from IEM subjects.

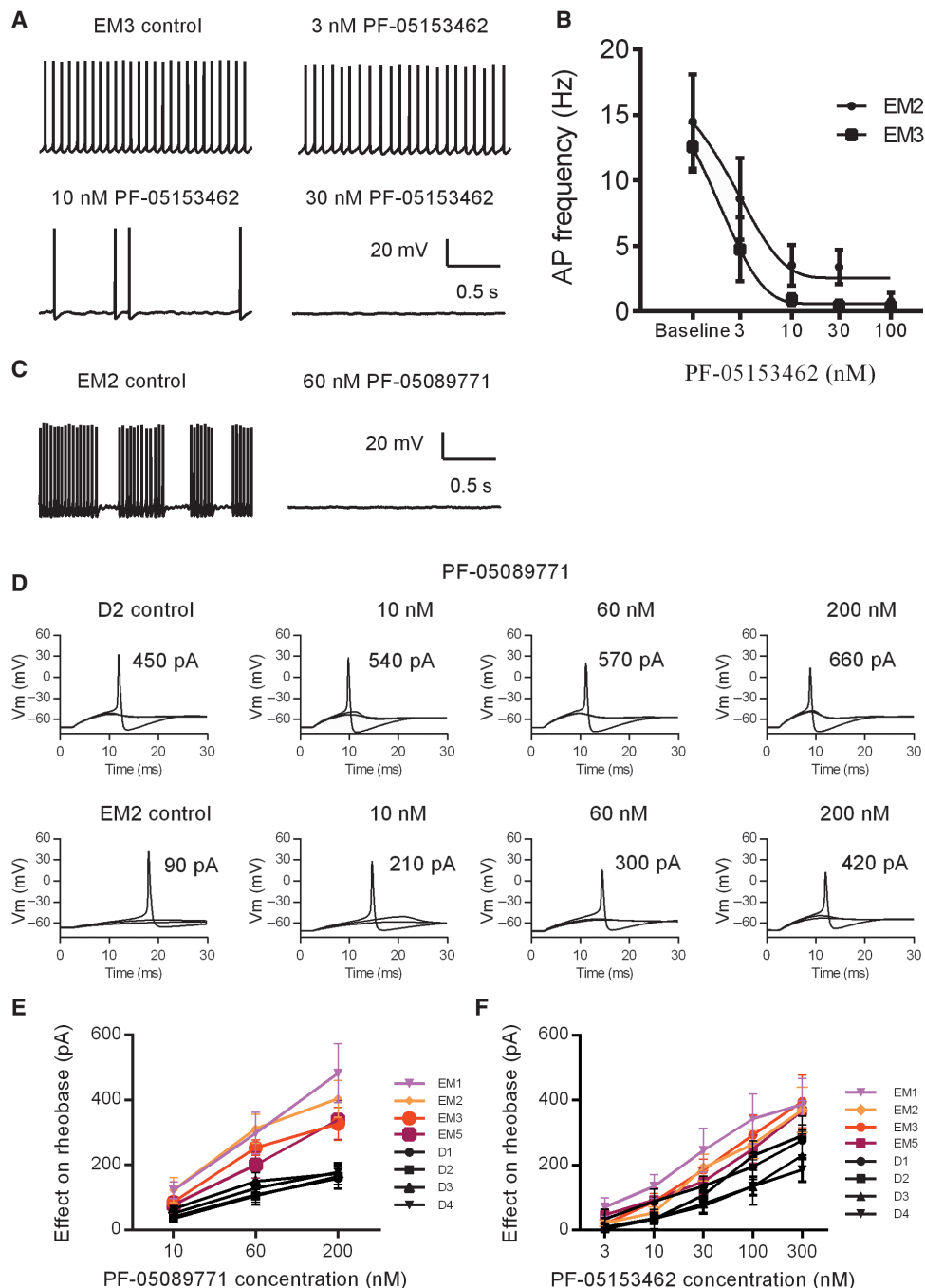
### Selective Nav1.7 blocker reverses the elevated sensitivity to heat in IEM iPSC-SNs

Action potential rheobase was tracked when the temperature was raised from  $35^{\circ}$  to  $40^{\circ}\text{C}$  (Fig. 4, A and B). In contrast to iPSC-SNs from the non-IEM donor group, the iPSC-SNs from the IEM subject group exhibited a significant decrease in rheobase in response to the modest temperature

increase ( $P < 0.01$ , ANOVA;  $n = 13$  to  $34$ ), indicating higher excitability of the IEM neurons upon heat stimulation. EM1 appeared to be an outlier with similar temperature sensitivity to healthy donor clones. These data suggested that the gain-of-function Nav1.7 mutations in the iPSC-SNs from IEM subjects conferred an increase in excitability in response to heating at innocuous temperatures. As shown in Fig. 4 (C and D),  $100$  nM PF-0515462 was able to reverse the effect of increasing temperature on the rheobase in iPSC-SNs from subjects EM2 (I848T mutation), EM3 (V400M mutation), and EM5 (F1449V mutation) ( $P < 0.05$ ,

### Fig. 3. Nav1.7 channel blockers reduce spontaneous firing and increase action potential rheobase in iPSC-SNs.

(A) Representative traces of spontaneous action potentials in IEM subject EM3 (V400M mutation) iPSC-SNs blocked by increasing concentrations of the Nav1.7 blocker PF-05153462. (B) Concentration-dependent effect of PF-05153462 on spontaneous action potential (AP) firing with a half-maximal inhibitory concentration ( $IC_{50}$ ) of 2 nM for iPSC-SNs from IEM subjects EM2 (I848T mutation) and EM3 (V400M mutation). (C) Representative traces of spontaneous firing blocked by treatment of iPSC-SNs from IEM subject EM2 with 60 nM PF-05089771. (D) Representative current-clamp traces in iPSC-SNs from non-IEM control subject D2 and IEM subject EM2 (I848T mutation) showing an increase in rheobase after application of PF-05089771 in a concentration-dependent manner. (E) Quantification of the effect of PF-05089771 on rheobase for iPSC-SNs from non-IEM control subjects and IEM subjects ( $n = 6$  to  $10$ ;  $P < 0.05$ , ANOVA). (F) Quantification of the effect of PF-05153462 on rheobase for iPSC-SNs from non-IEM control subjects and IEM subjects ( $n = 6$  to  $10$ ;  $P < 0.05$ , ANOVA; comparison at each concentration greater than 10 nM).



paired  $t$  test;  $n = 6$  to  $11$ ) in cells with a positive rheobase response ( $>50$  pA) to PF-05153462 at  $35^{\circ}\text{C}$  (an indication of the functional expression of Nav1.7). These data suggest that mutations in Nav1.7 underlie the temperature sensitivity of IEM iPSC-SNs.

The change in temperature sensitivity after compound application was plotted against the effect of compound on rheobase at  $35^{\circ}\text{C}$  (Fig. 5), and a positive correlation was observed in iPSC-SNs from all EM subjects (Pearson's  $r = 0.22, 0.88, 0.82,$  and  $0.77$  for EM1, EM2, EM3, and EM5, respectively). The regression coefficients were significantly different from zero for iPSC-SNs from subjects EM2 (I848T mutation), EM3

(V400M mutation), and EM5 (F1449V mutation), suggesting that the amplitude of rheobase changes in response to heat was a function of available Nav1.7 conductance. This effect was not evident in iPSC-SNs from subject EM1. Wild-type Nav1.7 channels were also sensitive to changes in temperature (fig. S4). Together, this analysis suggests that Nav1.7 channels contribute to the elevated heat sensitivity of IEM iPSC-SNs.

**Clinical efficacy of the selective Nav1.7 blocker PF-05089771**  
IEM subjects were randomized to participate in two independent treatment sessions (each consisting of two study periods) and to receive a

**Fig. 4. Nav1.7 channel blocker reverses the elevated heat sensitivity of iPSC-derived sensory neurons from IEM subjects.**

(A) Representative traces of evoked action potentials showing a small increase in rheobase when iPSC-SNs from non-IEM control subject D3 were incubated with extracellular recording solution at an elevated temperature of 40°C (control temperature was 35°C). The rheobase for iPSC-SNs for IEM subject EM5 (F1449V mutation) was decreased relative to the D3 control. Far right panels show an example time course for rheobase changes of iPSC-SNs from non-IEM subject D3 and IEM subject EM5 (F1449V mutation) upon heating of the incubation solution. (B) Quantification of the effect of heating on rheobase for non-IEM and IEM iPSC-SNs. The heating effect was calculated as the change in the rheobase at 40°C versus 35°C ( $n = 13$  to 34;  $P < 0.01$ , comparing non-IEM and IEM iPSC-SNs using ANOVA). (C) Representative traces of rheobase showing the effect of heating on rheobase before and after the application of the Nav1.7 channel blocker PF-05153462. The heat sensitivity of rheobase was reversed by PF-05153462 on iPSC-SNs from IEM subject EM5, but no effect was seen on iPSC-SN from IEM subject EM1.

(D) Quantification of the effect of PF-05153462 on heat sensitivity of iPSC-SNs from IEM subjects EM1 (S241T mutation), EM2 (I848T mutation), EM3 (V400M mutation), and EM5 (F1449V mutation) ( $n = 6$  to 10;  $P < 0.05$  for EM1, EM2, and EM5 and  $P < 0.01$  for EM3; paired  $t$  test). Only iPSC-SNs demonstrating a positive response to PF-05153462 (where the rheobase showed sensitivity greater than 50 pA at 35°C) were included, and the number of iPSC-SNs excluded was 3 of 12 iPSC-SNs for IEM subject EM1, 2 of 10 iPSC-SNs for IEM subject EM2, 1 of 8 iPSC-SNs for IEM subject EM3, and 1 of 11 iPSC-SNs for IEM subject EM5.

single oral dose of either the Nav1.7 blocker PF-05089771 or matched placebo in a crossover manner during each session. Evoked pain attacks were induced in subjects using a controlled heat stimulus applied to the extremities immediately before dosing and at intervals up to 24 hours after dosing in each study period (Fig. 6A). Blood samples collected from subjects for pharmacokinetic analysis showed that peak plasma concentrations of PF-05089771 were obtained at 4 to 6 hours after dosing (fig. S5). Mean unbound plasma concentrations of PF-05089771 at 4 and 6 hours after dosing were 166 and 161 nM, respectively.

Subjects rated their pain using a pain intensity numerical rating scale (PI-NRS) where 0 indicates no pain and 10 indicates the worst pain possible. A pain attack with a PI-NRS score of at least 5 was evoked before dosing with PF-05089771 or placebo. Efficacy end points included the average and maximum pain scores in response to evoked heat at 0 to 4, 4 to 5, 8 to 9, and 24 to 25 hours after dosing.

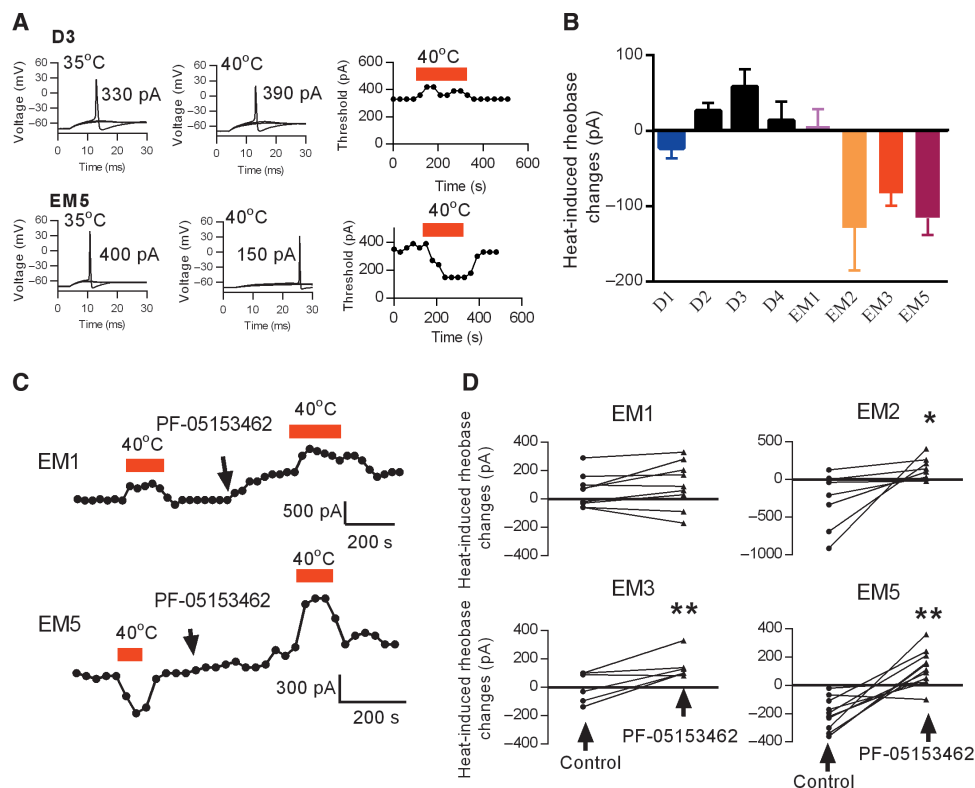
Individual subject maximum pain scores and change from baseline pain scores after dosing are shown in Fig. 6 (B and C). Maximum pain score results after dosing (Fig. 6D) were similar, irrespective of whether cooling rescue therapy [used by subjects EM2 (I848T mutation) and EM4 (V400M mutation)] was administered in the interval before evoking a pain attack. There was statistical significance for PF-05089771 versus placebo at the 10% level at the 4- to 5- and 8- to 9-hour time points after dosing. The  $P$  values for the comparison of PF-05089771 versus placebo were  $P = 0.04$  at 4 to 5 hours and  $P = 0.08$  at 8 to 9 hours when subjects who used cooling as a rescue therapy were excluded. When subjects who used cooling as a rescue therapy were included, the

corresponding  $P$  values were 0.06 and 0.03. There was no statistically significant treatment effect for PF-05089771 versus placebo at the 0- to 4-hour time point. PF-05089771 was well tolerated in all subjects, with all treatment-related adverse events classified as mild. The most common treatment-related adverse events were perioral paresthesia, facial flushing, and dizziness (table S1).

## DISCUSSION

Human iPSC-derived disease models can be used for the identification or validation of drugs to treat specific disease phenotypes (15, 16), yet the degree of translation of drug efficacy to the clinical disease state remains unexplored. Here, we show translation of a human pain phenotype and clinical effects of a new selective Nav1.7 blocker to the pre-clinical iPSC-based disease model from a small cohort of IEM subjects harboring different mutations in the *SCN9A* gene.

The IEM subject cohort had four different mutations in *SCN9A* and exhibited pain with multiple characteristics, making it an ideal population for a qualitative, proof-of-concept translational study to assess both phenotype and its reversal through selective Nav1.7 blockade. The Nav1.7 blocker used, PF-05089771, shows greater selectivity for Nav1.7 over all other sodium channel isoforms compared to other sodium channel blockers such as carbamazepine (17) and XEN402 (18, 19). A well-controlled heat stimulus triggered pain attacks in the IEM subject cohort and reproduced many of the features of a natural heat-evoked



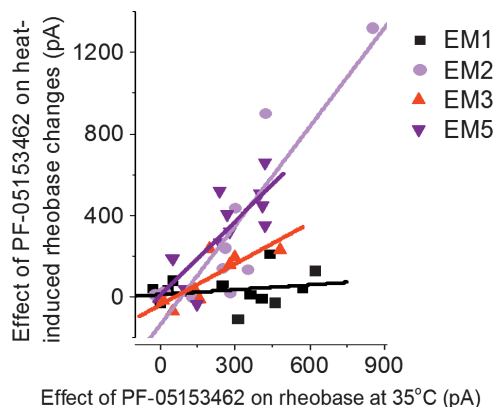


**Fig. 5. Nav1.7 contributes to the elevated heat sensitivity of iPSC-SNs from IEM subjects.** Correlation of the heat sensitivity changes to rheobase changes at 35°C induced by PF-05153462 (Pearson's  $r = 0.22, 0.88, 0.82,$  and  $0.77$  for IEM subjects EM1, EM2, EM3, and EM5, respectively). The regression coefficients were significantly different from zero for IEM subjects EM2, EM3, and EM5. In contrast to Fig. 4D, iPSC-SNs demonstrating a positive response to PF-05153462 (rheobase changes at 35°C greater than 50 pA, indicating clear Nav1.7 expression) and iPSC-SNs demonstrating a negative response to PF-05153462 (rheobase changes at 35°C less than 50 pA, indicating low or no Nav1.7 expression) were included.

pain attack (4). The magnitude of heat-induced pain attacks at 4 to 5 and 8 to 9 hours after dosing was reduced in most of the five subjects during at least one of the treatment sessions when dosed with PF-05089771 compared to subjects who received placebo, confirming efficacy in this proof-of-concept study for the treatment of IEM with a selective Nav1.7 blocker. The shorter duration of the evoked pain attacks [usually less than 1 hour compared to the longer duration recorded in the natural history study (4)] and the time of maximum concentration ( $T_{max}$ ) of PF-05089771 after dosing may account for the lack of treatment response at the 0- to 4- and 24- to 25-hour time points. There appeared to be a degree of variability in response across subjects and between treatment sessions. These observations may be accounted for by the limitation of a single-dose study. iPSCs derived from these subjects provided a unique means to directly evaluate the efficacy of PF-05089771 blockade on the phenotypes of these channel mutations in human sensory neurons.

The increased excitability of iPSC-SNs from IEM subjects was not associated with increased expression of Nav1.7 sodium channels; however, the mean resting membrane potential of iPSC-SNs from IEM subjects was moderately depolarized compared to neurons from the non-IEM donor group. This elevated excitability is likely to be due to an increase in Nav1.7 subthreshold current as modeled by Vasylyev *et al.* (20). Overexpression of the F1449V, V400M, I848T, and S241T Nav1.7 mutations in rodent dorsal root ganglion neurons has also been reported to reduce current threshold and increase the frequency of firing of dorsal root ganglion neurons in response to graded stimuli (21–23). The pathophysiological consequence of IEM on neuronal excitability has been examined in clinical microneurography studies (24, 25). One subject with the I848T mutation demonstrated increased C-fiber nociceptor excitability (26). The microneurography recordings from human nerves and the excitability measurements in iPSC-SNs from patients carrying the same Nav1.7 mutation (I848T) support a role for sensory neuron hyperexcitability underlying the symptoms of IEM.

Direct proof for a role of Nav1.7 in hyperexcitability of sensory neurons from IEM subjects was provided by two Nav1.7 blockers. Both of these compounds have a greater effect on the rheobase of iPSC-SNs from the IEM subject group compared to the non-IEM donor group, and both compounds reduced spontaneous activity of iPSC-SNs from IEM subjects. These data demonstrate using native human Nav1.7 channels in human-derived sensory neurons that Nav1.7 mutations associated with IEM lead to a gain-of-function phenotype.

Of particular interest is subject EM1 (S241T mutation). The iPSC-SNs from this subject were less excitable than other iPSC-SNs from the other IEM subjects in the study, yet the effect of the Nav1.7 blockers on rheobase was equivalent across all IEM iPSC-SNs, confirming the Nav1.7 gain-of-function phenotype. Furthermore, although most IEM patient-derived neurons were more excitable in response to heat in accordance with the clinical phenotype, PF-05153462 only blocked the heat-evoked response in EM2 (I848T mutation)–, EM3 (V400M mutation)–, and EM5 (F1449V mutation)–derived sensory neurons, demonstrating that these Nav1.7 mutations contribute to enhanced temperature sensitivity. In contrast, there was no effect of temperature on EM1 (S241T mutation). It is possible that the lack of response of heat-evoked pain in EM1 (S241T mutation) to PF-05089771 in the clinical study was related to the lack of Nav1.7 temperature dependence at the temperatures tested in iPSC-SNs. Age of IEM onset was delayed (17 years old) in subject EM1 (S241T mutation) compared to the other IEM subjects. Previously published studies also report that for the S241T mutation, the age of onset was between 8 and 10 years old [for four of six affected family members (27)] in comparison to early onset (from infancy until 6 years old) with mutations V400M, F1449V, and I848T (17, 21). IEM mutations in patients with delayed onset are associated with smaller shifts in channel gating and reduced hyperexcitability compared to mutations associated with onset in early childhood (22).

The lower excitability of sensory neurons derived from iPSCs from subject EM1 carrying the S241T mutation may reflect the delayed onset of IEM, either due to differences in Nav1.7 biophysics or different processing of Nav1.7 during cell maturation relative to the other IEM mutant Nav1.7 channels. It is not appropriate to draw a clear cause and effect relationship between the complex individual subject clinical phenotype and the phenotype of the cognate iPSC-SNs; nevertheless, it is interesting to note that subject EM1 (S241T mutation) had the mildest clinical phenotype, and the iPSC-SNs derived from this patient were the least excitable of the IEM-derived cell lines. In contrast, subject EM2 (I848T mutation) had a more severe clinical phenotype and their iPSC-SNs were highly excitable. With this apparent translation of phenotype and treatment response from clinical study subject to the cognate iPSC disease model, it will be interesting to further decipher underlying mechanisms of this variability. It is also interesting to note the range of excitability within the iPSC-SNs from the four non-IEM donors. Further studies are required to determine the degree of variation in excitability of sensory neurons across the normal human population and its biological basis.

Our data demonstrate the utility of Nav1.7 blockers for the treatment of pain caused by IEM and the utility of iPSC-SNs for recapitulation of sensory nerve fiber dysfunction in vitro. Our results also highlight differences in the effect of the clinical compound in cells derived from non-IEM donors relative to IEM subjects. Thus, iPSC-SNs may further assist in the understanding of certain pain conditions and potential pharmacoresponsiveness of individuals to established and new treatments.

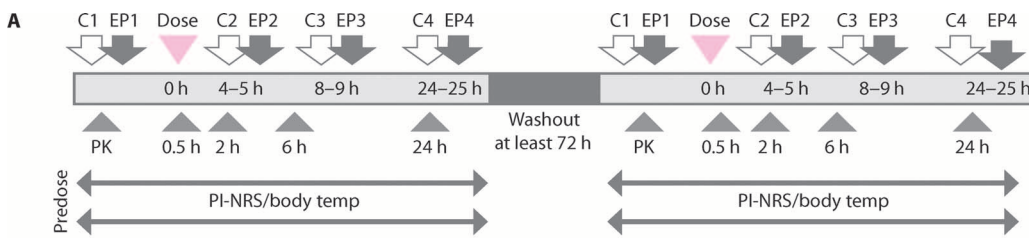
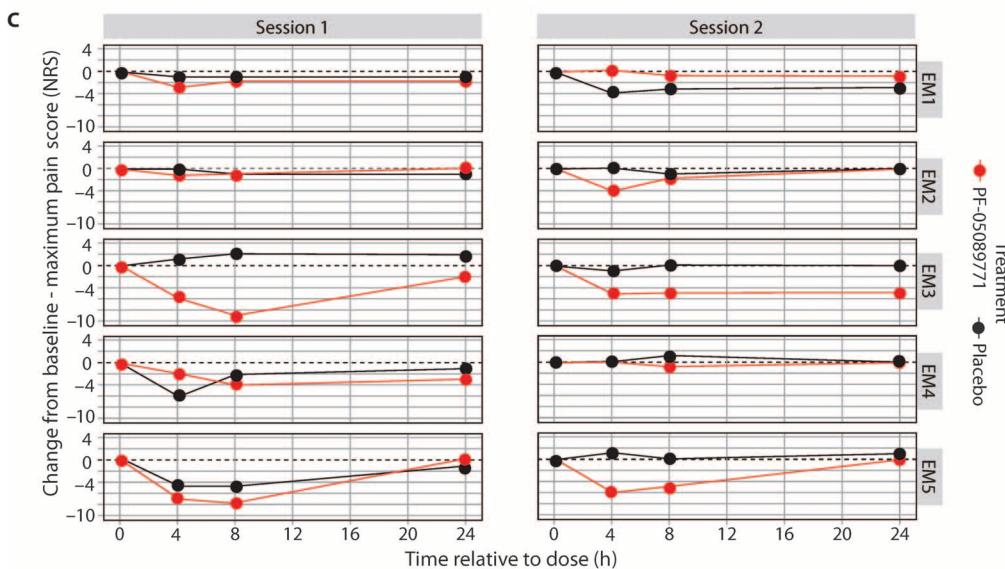
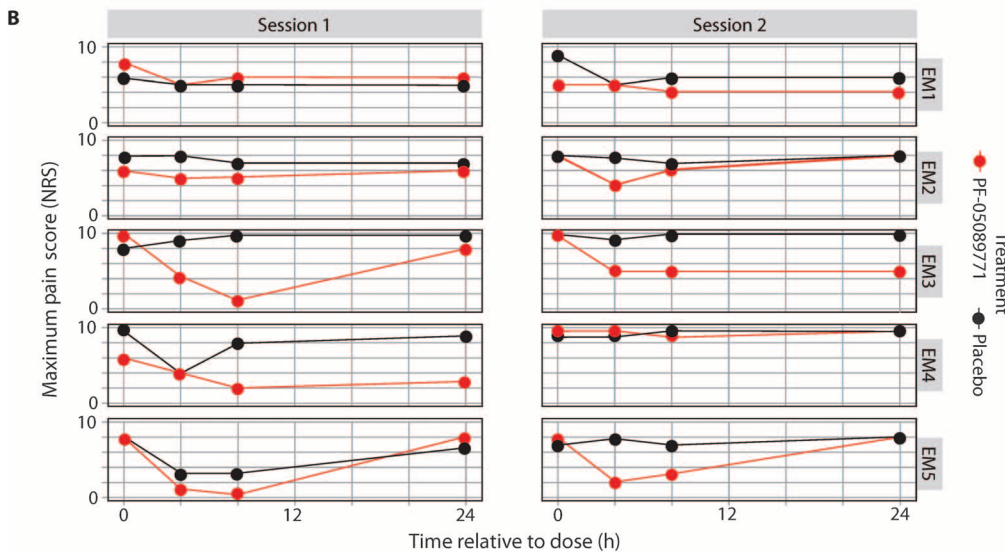


**Fig. 6. Clinical study design overview and maximum pain scores after dosing.** (A) Each treatment session consisted of two study periods separated by at least a 72-hour washout period. Subjects received either a single oral dose of the Nav1.7 channel blocker PF-05089771 or placebo in a crossover manner in each study period. Pain scores were recorded every 15 min up to 10 hours after dosing. Core body temperature was measured regularly throughout the study period. The cooling paradigm (C1 to C4) was used before evoking pain (EP1 to EP4) at specific time points during the study period. Pharmacokinetic (PK) samples were collected before dosing and at 0.5, 2, 6, and 24 hours after dosing. (B) Maximum pain scores recorded by subjects using the PI-NRS after dosing with either the Nav1.7 channel blocker PF-05089771 or placebo in TS1 and TS2. Individual subject results for maximum pain scores included subjects who used non-pharmacological cooling therapy to alleviate pain. IEM subject EM1 (S241T mutation) did not show any notable difference in pain scores after PF-05089771 treatment compared to placebo between TS1 and TS2. IEM subject EM2 (I848T mutation) had a reduction in pain scores in TS2 after PF-05089771 treatment compared to placebo at the 4- to 5-hour postdose time point. IEM subject EM4 (V400M mutation) had a reduction in pain score at the 4- to 5- and 8- to 10-hour postdose time point in TS1, but no difference in pain scores between drug and placebo in TS2. IEM subjects EM3 (V400M mutation) and EM5 (F1449V mutation) had a reduction in pain scores after a single dose of PF-05089771 at the 4- to 5-hour time point and the 8- to 10-hour postdose time point in both TS1 and TS2. (C) Change from baseline in maximum pain scores (PI-NRS) after PF-05089771 treatment versus placebo in individual IEM subjects. (D) Differences in maximum pain scores after dosing with PF-05089771 including and excluding IEM subjects who used cooling as “rescue” therapy.



Differences in maximum pain scores postdose (includes/excludes cooling rescue therapy)						
Time postdose	P value	Treatment difference (PF-05089771 - placebo)	90% confidence interval	P value	Treatment difference (PF-05089771 - placebo)	90% confidence interval
0-4 h	0.49	-0.33	-1.17, 0.51	0.74	0.25	-1.17, 1.67
4-5 h	0.06	-2.56	-4.74, -0.39	0.04	-3.13	-5.43, -0.82
8-9 h	0.03	-3.63	-6.24, -1.01	0.08	-3.63	-6.91, -0.34
24-25 h	0.47	-0.77	-2.84, 1.29	0.47	-0.77	-2.84, 1.29

There are, however, some limitations to this work. IEM is a rare disease; as a result, the number of eligible subjects in the clinical study was small, representing four different mutations. Because the study involved a single dose of compound, it was not possible to generate dose-response information. The free plasma concentrations of PF-05089771 in the clinical study reached magnitudes that would have been expected to fully inhibit Nav1.7 activity. Given the selectivity profile of the compound, there may also have been limited activity at other peripherally expressed sodium channels, such as Nav1.6. Prior to use in clinical practice, these results may need to be extended to additional IEM subjects, particularly those with *SCN9A* gain-of-function mutations that have not been characterized in the current study. Future studies may also look to extend these results to other *SCN9A*-associated pain conditions such as paroxysmal extreme pain disorder and idiopathic small fiber neuropathy. In addition, it may be possible to extend these results to more general chronic pain conditions in which *SCN9A* mutations associated with a gain of function of the Nav1.7 channel may contribute to the pain in subgroups of subjects.

In summary, this study demonstrates the utility of iPSC technology to bridge the gap between clinical and preclinical studies, enabling an understanding of both the disease and the response to a therapeutic agent.

## MATERIALS AND METHODS

### Study design

The clinical study was a two-part, randomized, double-blind, third-party open, placebo-controlled exploratory crossover study conducted at a single study site. Eligible subjects were adult males or females with clinically and genetically characterized IEM. Subjects were randomized to receive a single oral dose of either PF-05089771 or placebo in a 1:1 ratio during each study period. PF-05089771 and placebo doses were closely matched to maintain the blindedness of the study. All subjects provided informed consent in accordance with ethical principles originating or derived from the Declaration of Helsinki 2008 before undergoing study-related procedures. This study was reviewed and approved by an Independent Ethics Review Board. Because of the rarity of IEM, sample sizing for the study was originally based on enrollment of up to 14 subjects. The study was powered such that there was an 80% chance of meeting the decision criteria if the true difference in average 0- to 4-hour pain scores was 1.4. The decision criterion was a Bayesian probability of at least 0.75 of the true difference greater than 0.6.

### Clinical study

Subjects were excluded from the clinical study if they had other clinically significant illnesses or were unable to wash out of and refrain from using concomitant pain medications during the study such as carbamazepine, lamotrigine, oxcarbazepine, mexiletine and amitriptyline, capsaicin patches and local anesthetic patches, and oral/injectable corticosteroids. All subjects washed out of their concomitant pain medications before taking part in the study. To manage pain due to their IEM during the study, subjects were permitted to use nonpharmacological therapy such as cooling the extremities or acetaminophen (up to a maximum of 3000 mg/day).

The five subjects enrolled in this study had participated in a previous nondrug clinical phenotyping study in which the triggers for pain attacks and the duration, intensity, and frequency of pain attacks and

ongoing pain between attacks (if any) were recorded by subjects in a pain diary on a daily basis over a 3-month period. Pain attacks occurred primarily in the feet and hands, and the principal triggers for evoking pain attacks were warmth or heat, exercise, and environmental factors (usually hot and/or humid weather) (4).

The primary objective of the drug study was to evaluate the overall pain intensity over 4 hours after a single 1600-mg oral dose of PF-05089771 against placebo in subjects experiencing either experimentally evoked (heat stimulation) pain or spontaneous pain due to IEM. The secondary objectives of the study were to evaluate the overall duration, maximum pain intensity, and duration of pain intensity (evoked or spontaneous pain) in subjects at 4 to 5, 8 to 9, and 24 to 25 hours after dosing. Use of and time to use of pharmacological therapy such as acetaminophen or nonpharmacological therapy such as cooling the extremities to relieve IEM pain during the study ("rescue therapy") were also recorded.

Part A, the first part of the study, was conducted over 1 to 2 days as an in-clinic stay to establish clinical reproducibility and reliability of evoking pain in each subject before entering part B, an extended in-clinic stay in which a single oral dose of study drug or matched placebo was administered. Subjects were randomized into part B of the study provided that they satisfied all subject selection criteria and had a self-reported spontaneous or evoked pain score of  $\geq 5$  on the PI-NRS (where 0 indicates no pain and 10 indicates worst pain possible) before dosing. Treatment session 1 (TS1) and TS2 could be run consecutively, with a minimum 72-hour washout period between the last study treatment in TS1 and the first study treatment in TS2, and a maximum period of up to 6 months between TS1 and TS2 to facilitate enrollment.

The Medi-Therm III MTA 7900 (Stryker) device was used as a heating device to evoke pain, as a cooling device for the cooling paradigm part of the study, and as means to deliver nonpharmacological cooling of the extremities as rescue therapy. The Medi-Therm device supplied cold or warm water at operator-determined temperatures through the use of water-circulating thermo-regulated blankets applied to the feet and/or hands or body wraps, which were applied to the trunk. The hands and feet, including toes, were completely enclosed in the thermal blankets, which were applied in a consistent manner to each subject. Subjects rated their baseline pain score using the PI-NRS. If the subject reported any ongoing pain, attempts were made to reduce the subject's pain score to  $\leq 3$  on the PI-NRS using a cooling paradigm. Thermal blankets were applied to the subject's extremities (feet and/or hands), and the Medi-Therm blankets cooled to 20°C (cooling paradigm) for at least 5 min (maximum of 60 min) until the subject's pain score was  $\leq 3$  on the NRS. After cooling, the thermal blankets were heated to 33°C, the starting temperature for all subjects, and the temperature was increased incrementally in 1° to 2°C steps at 10- to 15-min intervals to the device maximum of 42°C. This temperature was used for a maximum duration of 30 min, until a pain attack with a PI-NRS score of  $\geq 5$  was induced. This methodology was repeated at least one to two times in part A of the study to establish individual, standardized time and temperature parameters for evoking pain in each subject for part B, the drug phase of the study. Subjects recorded pain scores every 15 min for up to 4 hours after a pain attack was evoked.

Part B of the study had two treatment sessions (TS1 and TS2) with each treatment session consisting of two study periods (Fig. 6A). Subjects received a single dose of either PF-05089771 or placebo in each study period. Treatment sessions could be carried out consecutively, with a minimum washout period of at least 72 hours between study treatments, or separated by up to 6 months. In part B, subjects' extremities

were cooled (C1 to C4; Fig. 6A) to reduce pain score to  $\leq 3$  on the NRS, followed by heat stimulation to evoke a pain attack (EP1 to EP4). Once the subject reported a pain score of  $\geq 5$  on the PI-NRS, as a result of the Medi-Therm device heat stimulus, they were randomized to one of two double-blind treatment sequences [PF-05089771/placebo or placebo/PF-05089771, each given as a single oral dose during each of the treatment sessions (TS1 and TS2)]. To maintain blinding, PF-05089771 and placebo oral doses were matched in appearance and volume. Postdose pain attacks were evoked, using individual standardized parameters established in part A with the Medi-Therm device, at 4 to 5, 8 to 9, and 24 to 25 hours after dosing. Subjects were asked to refrain from taking acetaminophen or nonpharmacological treatments (for example, Medi-Therm cooling function, ice buckets, cold water, and cool air fans) to manage pain until at least 90 min after dosing. If acetaminophen or cold therapy were requested by the subject to manage pain, the time, dose (where applicable), duration, and frequency of use were recorded. Pain scores were recorded every 5 min for the first hour after dosing and then every 15 min until 10 hours after dosing. Blood samples were collected for pharmacokinetic and safety laboratory evaluations at pre-specified time points after dosing. Blood and urine samples for laboratory assessments (hematology, serum chemistry, and urinalysis) were collected 2 days before dosing, at 2 to 4 hours before dosing, and at 24 hours after dosing in each study period. Vital signs were checked 2 days before dosing, at 2 to 4 hours before dosing, and at 6 and 24 hours after dosing. Electrocardiograms were performed 2 days before dosing, at 2 to 4 hours before dosing, and at 8 and 24 hours after dosing. Adverse events were recorded at the time of occurrence from screening until follow-up (28 days after the last dose of study drug).

### Collection of blood for generation of iPSCs

Four of five subjects (EM1, EM2, EM3, and EM5) consented to an optional procedure to donate blood for generation of iPSCs. About 60 ml of blood was collected per subject and aliquoted into six 8-ml Ficoll CPT tubes with sodium heparin (Becton Dickinson). The samples were centrifuged at room temperature, and mononuclear cells (lymphocytes and neutrophils) were harvested and further centrifuged. The centrifuged cells were aspirated and counted using a hemocytometer. Trypan blue was used to identify nonviable cells. Viable cells were resuspended in freezing solution (human AB serum plus 10% dimethyl sulfoxide) to give a final cell density of not more than 50 million cells/ml. Samples were frozen at  $-80^{\circ}\text{C}$ .

### Clinical statistical methods

The primary end point, the average heat-evoked pain score from 0 to 4 hours after dosing was analyzed using a linear mixed model with terms for baseline, treatment period time after dosing, baseline by time after dosing interaction, treatment by time after dosing interaction, and period by time after dosing interaction. Subject was included as a random effect in this model. The secondary end points of maximum pain score following pain provocation at 4, 8, 10, and 24 hours after dosing were analyzed using a linear fixed effects model with additive terms for subject, period, and treatment. The results are summarized as estimates of treatment effects (PF-05089771 minus placebo) together with 90% confidence intervals. Maximum pain scores obtained after pain provocation following previous use of rescue therapy were included in the analyses because the rescue medication was nonpharmacological cooling, which was also used in the study design to cool subjects if necessary before pain provocation.

### Generation and maintenance of iPSCs derived from IEM subjects

Blood samples from non-IEM donors were obtained from the National Health Service Blood and Transplant (NHSBT). Samples from IEM clinical trial subjects were obtained after informed consent.

Peripheral blood mononuclear cells were purified using the standard Ficoll-Paque procedure. Cells were expanded into erythroid progenitor cells and transduced with Sendai virus expressing Yamanaka factors OKSM (Life Technologies). iPSC colonies were further expanded to virus-free clonal lines that were cultured and maintained on Matrigel (BD) in TeSR1 (STEMCELL Technologies) and passaged every 6 to 7 days using dispase (Life Technologies).

### Genomic DNA isolation, Sanger sequencing, and array CGH

Genomic DNA of IEM subject material and iPSC clones was extracted using Qiagen RNA/DNA isolation kit. Segments containing respective mutations were PCR amplified and sequenced for mutation analysis.

Primer sequences [IDT (Integrated DNA Technologies)] used were as follows: S241T forward, 5'-CATGACTTTCTAGGAAAGCTTGTGT-3'; S241T reverse, 5'-GTCCAATTAGTGCAAACACACTCA-3'; I848T forward, 5'-ATCATTGACTGCTCCGAGTCTT-3'; I848T reverse, 5'-TTGCAGACACATTCTTTGTAGCTC-3'; S449N forward, 5'-GGGTTTCCTAGGATTTGGAAATGAC-3'; S449N reverse, 5'-CTGATGCTGTCCCTCTGATTCTGAT-3'; V400M forward, 5'-ATTTCCATTTTTCCCTAGACGCTG-3'; V400M reverse, 5'-TACCTCAGCTTCTTCTTGCTCTTT-3'; F1449V forward, 5'-TTATAGGTAGACAAGCAGCCCAAA-3'; F1449V reverse, 5'-CCTA-AATCATAAGTTAGCCAGAACC-3'. Array CGH analysis was performed with genomic DNA of iPSC clones and corresponding subject material using CytoSure ISCA v2 4  $\times$  180k microarrays and analyzed using CytoSure software (Oxford Gene Technology).

### RNA isolation, complementary DNA synthesis, and qPCR

Total RNA of cells was isolated using the RNeasy Mini Kit (Qiagen) and reverse-transcribed using SuperScript III complementary DNA synthesis kit (Life Technologies) according to the manufacturer's protocol. qPCR was performed using the TaqMan Gene Expression system (Applied Biosystems). The TaqMan probes (Life Technologies) used were SCN1A, Hs00374696\_m1; SCN2A, Hs00221379\_m1; SCN3A, Hs00366902\_m1; SCN4A, Hs01109480\_m1; SCN8A, Hs00274075\_m1; SCN9A, Hs0161567\_m1; SCN10A, Hs01045149\_m1; SCN11A, Hs00204222\_#m1; GAPDH, Hs02758991\_#g1; and HPRT, Hs02800695\_m1.

### Immunocytochemistry

iPSC clones or sensory neurons were fixed in 4% paraformaldehyde for 20 min at room temperature, permeabilized in 0.3% Triton X-100 in phosphate-buffered saline (PBS), and blocked with 5% donkey serum/PBS-0.1% Triton X-100 (PBS-T). iPSC clonal lines were stained with primary antibodies anti-Oct4 (sc-8628, Santa Cruz Biotechnology) and anti-Nanog (ab62734, Abcam) overnight. Sensory-like neurons were stained with anti-peripherin, anti-Brn3a, and anti-Islet1 (sc-7604, Santa Cruz Biotechnology; ab5945 and ab86501, Abcam) overnight. Cells were incubated with Alexa fluorophore secondary antibodies (Life Technologies) in PBS-T for 1 hour with intermediate washes. Nuclei were stained with Hoechst (Life Technologies). Images were acquired on the Zeiss Observer ZI with AxioVision software (Zeiss) or ImageXpress platform (Molecular Devices).

## Differentiation of iPSCs into sensory neurons

Differentiation into sensory neurons was performed as described previously (13, 14). Differentiated neurons were maintained for 8 weeks in neural growth factor medium containing Dulbecco's modified Eagle's medium/F12 (1:1) supplemented with 10% fetal bovine serum (Life Technologies) and nerve growth factor (10 ng/ml), brain-derived neurotrophic factor (BDNF), glial cell line-derived neurotrophic factor (GDNF), neurotrophin-3 (NT-3) (PeproTech), and ascorbic acid (Sigma-Aldrich). Medium was changed twice weekly.

## Electrophysiology

iPSC-SNs (typically 8 weeks after growth factor addition) were dissociated and replated as described by Chambers *et al.* (13). Patch-clamp experiments were performed in whole-cell configuration using a patch-clamp amplifier (200B) for voltage clamp and MultiClamp (700A or 700B) for current clamp controlled by pCLAMP 10 software (Molecular Devices). Voltage-clamp experiments were performed at room temperature, whereas current-clamp experiments were performed at 35° or 40°C using a CL-100 in-line solution heating system (Warner Instruments).

Temperature was calibrated at the outlet of the in-line heater before each experiment. Patch pipettes had resistances between 1.5 and 2 megohms. Basic extracellular solution contained 135 mM NaCl, 4.7 mM KCl, 1 mM CaCl<sub>2</sub>, 1 mM MgCl<sub>2</sub>, 10 mM Hepes, and 10 mM glucose (pH was adjusted to 7.4 with NaOH). The intracellular (pipette) solution for voltage clamp contained 100 mM CsF, 45 mM CsCl, 10 mM NaCl, 1 mM MgCl<sub>2</sub>, 10 mM Hepes, and 5 mM EGTA (pH was adjusted to 7.3 with CsOH). For current-clamp experiments, the intracellular (pipette) solution contained 130 mM KCl, 1 mM MgCl<sub>2</sub>, 5 mM MgATP, 10 mM Hepes, and 5 mM EGTA (pH was adjusted to 7.3 with KOH). The osmolality of solutions was adjusted to 320 mosmol/liter for extracellular solution and 300 mosmol/liter for intracellular solutions. All chemicals were purchased from Sigma-Aldrich. Currents were sampled at 20 kHz and filtered at 5 kHz. In voltage-clamp recordings, between 80 and 90% of the series resistance was compensated to reduce voltage errors. The voltage protocol used to assess the effect of the compounds on voltage-gated sodium channels consisted of a step to -70 mV for 5 s from a holding potential of -110 mV, followed by a recovery step to -110 mV for 100 ms, followed by a test pulse to 0 mV lasting 20 ms. Intersweep intervals were 15 s. Current threshold (or rheobase) was measured in current-clamp mode by injecting 30-ms duration current steps of regularly increasing amplitude until a single action potential was evoked. The increasing current steps were in cycled sweeps to track the changes of current threshold (rheobase) while temperature was varied or compounds were applied to the cells. Intersweep intervals were 2 s. Two to three subclones were generated for each of the four IEM donors and four healthy donors. Excitability data were pooled from all subclones of four IEM donors (individual subclones data can be seen in fig. S3D), whereas one subclone of each healthy donor was investigated.

Excitability was measured at resting membrane potential for each cell. The effect of compounds and temperature on rheobase was measured at a fixed membrane potential of -70 mV to avoid membrane potential change-induced error. Current-clamp data were analyzed using Spike2 software (Cambridge Electronic Design), Prism 6.0 (GraphPad software), and Origin 9.1 software (OriginLab). Wherever possible, the raw or derived data are presented.

## Statistical analysis

**Preclinical data.** Nonparametric ANOVA was used to compare current densities, total sodium current, and rheobase between the IEM and non-IEM groups of clones. Spontaneous action potential firing was analyzed using a linear logistic model to compare the IEM and non-IEM groups. Resting membrane potential and rheobase of the action potential were analyzed using ANOVA to compare between groups. Pearson's correlation coefficients were calculated to summarize the relationships between change in temperature sensitivity and effect on rheobase. The associated regression coefficients were tested to see if they differed significantly from zero. All significance tests were one-sided and used a 5% significance level. No adjustments were made to this significance level. Distributional assumptions were checked graphically, and when violated, nonparametric tests were used. All statistical analyses were carried out using SAS 9.4 (SAS Institute Inc.).

**Clinical data.** The primary end point, the average heat-evoked pain score from 0 to 4 hours after dosing, was analyzed using a linear mixed model with terms for baseline, treatment period by time after dosing, baseline by time after dosing interaction, treatment by time after dosing interaction, and period by time after dosing interaction. Subject was included as a random effect in this model. The secondary end points of maximum pain score following pain provocation at 4, 8, 10, and 24 hours after dosing were analyzed using a linear fixed effects model with additive terms for subject, period, and treatment. The results are summarized as estimates of treatment effects (PF-05089771 minus placebo) together with 90% confidence intervals. Unadjusted exact *P* values were given for maximum pain results, whereas a one-sided 10% significance level was used to test for a difference in the average pain from 0 to 4 hours after dosing. Distributional assumptions for the analyses were checked graphically. Maximum pain scores obtained after pain provocation following previous use of rescue therapy were included in the analyses because the rescue medication was nonpharmacological cooling, which was also used in the study design to cool subjects if necessary before pain provocation.

## SUPPLEMENTARY MATERIALS

[www.sciencetranslationalmedicine.org/cgi/content/full/8/335/335ra56/DC1](http://www.sciencetranslationalmedicine.org/cgi/content/full/8/335/335ra56/DC1)

Fig. S1. Molecular karyotype of IEM and non-IEM iPSCs and Nav channel subtype mRNA expression in iPSC-SNs.

Fig. S2. Molecular structure and selectivity profiles of Nav1.7 channel blockers.

Fig. S3. Electrophysiological properties of IEM and non-IEM iPSC sensory neurons.

Fig. S4. Effect of PF-05153462 on heat sensitivity of non-IEM control D3 and D4 iPSC sensory neurons.

Fig. S5. Pharmacokinetic profile of PF-05089771 over time after single oral dose administration to subjects with IEM.

Table S1. Common adverse event profile for all five subjects with IEM.

## REFERENCES AND NOTES

- J. P. H. Drenth, S. G. Waxman, Mutations in sodium channel gene SCN9A cause a spectrum of human genetic pain disorders. *J. Clin. Invest.* **117**, 3603–3609 (2007).
- S. D. Dib-Hajji, Y. Yang, J. A. Black, S. G. Waxman, The Na<sub>v</sub>1.7 sodium channel: From molecule to man. *Nat. Rev. Neurosci.* **14**, 49–62 (2013).
- D. L. H. Bennett, C. G. Woods, Painful and painless channelopathies. *Lancet Neurol.* **13**, 587–599 (2014).
- A. McDonnell, B. Schulman, Z. Ali, S. D. Dib-Hajji, F. Brock, S. Cobain, T. Mainka, J. Vollert, S. Tarabar, S. G. Waxman, Inherited erythromelalgia due to mutations in SCN9A: Natural history, clinical phenotype and somatosensory profile. *Brain* **139** (Pt. 4), 1052–1065 (2016).
- T. R. Cummins, S. D. Dib-Hajji, S. G. Waxman, Electrophysiological properties of mutant Nav1.7 sodium channels in a painful inherited neuropathy. *J. Neurosci.* **24**, 8232–8236 (2004).

6. M.-T. Wu, P.-Y. Huang, C.-T. Yen, C.-C. Chen, M.-J. Lee, A novel *SCN9A* mutation responsible for primary erythromelalgia and is resistant to the treatment of sodium channel blockers. *PLoS One* **8**, e55212 (2013).
7. M. Estacion, Y. Yang, S. D. Dib-Hajj, L. Tyrrell, Z. Lin, Y. Yang, S. G. Waxman, A new  $Na_v1.7$  mutation in an erythromelalgia patient. *Biochem. Biophys. Res. Commun.* **432**, 99–104 (2013).
8. M. Eberhart, J. Nakajima, A. B. Klinger, C. Neacsu, K. Hühne, A. O. O'Reilly, A. M. Kist, A. K. Lampe, K. Fischer, J. Gibson, C. Nau, A. Winterpacht, A. Lampert, Inherited pain: Sodium channel  $Nav1.7$  A1632T mutation causes erythromelalgia due to a shift of fast inactivation. *J. Biol. Chem.* **289**, 1971–1980 (2014).
9. T. Stadler, A. O. O'Reilly, A. Lampert, Erythromelalgia Mutation Q875E Stabilizes the Activated State of Sodium Channel  $Nav1.7$ . *J. Biol. Chem.* **290**, 6316–6325 (2015).
10. E. C. Emery, A. M. Habib, J. J. Cox, A. K. Nicholas, F. M. Gribble, C. G. Woods, F. Reimann, Novel *SCN9A* mutations underlying extreme pain phenotypes: Unexpected electrophysiological and clinical phenotype correlations. *J. Neurosci.* **35**, 7674–7681 (2015).
11. J. W. Theile, B. W. Jarecki, B. W. A. D. Piekarz, T. R. Cummins,  $Nav1.7$  mutations associated with paroxysmal extreme pain disorder, but not erythromelalgia, enhance  $Nav\beta4$  peptide-mediated resurgent sodium currents. *J. Physiol.* **589**, 597–608 (2011).
12. S. D. Dib-Hajj, J. S. Choi, L. J. Macala, L. Tyrrell, J. A. Black, T. R. Cummins, S. G. Waxman, Transfection of rat or mouse neurons by biolistics or electroporation. *Nat. Protoc.* **4**, 1118–1126 (2009).
13. S. M. Chambers, Y. Qi, Y. Mica, L. Gabsang, X.-J. Zhang, L. Niu, J. Bilsland, L. Cao, E. Stevens, P. Whiting, S.-H. Shi, L. Studer, Combined small-molecule inhibition accelerates developmental timing and converts human pluripotent stem cells into nociceptors. *Nat. Biotechnol.* **30**, 715–720 (2012).
14. G. T. Young, A. Gutteridge, H. D. E. Fox, A. L. Wilbrey, L. Cao, L. T. Cho, A. R. Brown, C. L. Benn, L. R. Kammonen, J. H. Friedman, M. Bictash, P. Whiting, J. G. Bilsland, E. B. Stevens, Characterizing human stem cell-derived sensory neurons at the single-cell level reveals their ion channel expression and utility in pain research. *Mol. Ther.* **22**, 1530–1543 (2014).
15. M. Grskovic, A. Javaherian, B. Strulovici, G. Q. Daley, Induced pluripotent stem cells—Opportunities for disease modelling and drug discovery. *Nat. Rev. Drug Discov.* **10**, 915–929 (2011).
16. J. McNeish, J. P. Gardner, B. J. Wainger, C. J. Woolf, K. Eggan, From dish to bedside: Lessons learned while translating findings from a stem cell model of disease to a clinical trial. *Cell Stem Cell* **17**, 8–10 (2015).
17. T. Z. Fischer, E. S. Gilmore, M. Estacion, E. Eastman, S. Taylor, M. Melanson, S. D. Dib-Hajj, S. G. Waxman, A novel  $Na_v1.7$  mutation producing carbamazepine responsive erythromelalgia. *Ann Neurol.* **65**, 733–741 (2009).
18. Y. P. Goldberg, N. Price, R. Namdari, C. J. Cohen, M. H. Lamers, C. Winters, J. Price, C. E. Young, H. Verschoof, R. Sherrington, S. N. Pimstone, M. R. Hayden, Treatment of  $Nav1.7$ -mediated pain in inherited erythromelalgia using a novel sodium channel blocker. *Pain* **153**, 80–85 (2012).
19. Y. P. Goldberg, C. J. Cohen, R. Namdari, N. Price, J. A. Cadieux, C. Young, R. Sherrington, S. N. Pimstone, Letter to the Editor. *Pain* **155**, 837–838 (2014).
20. D. V. Vasylyev, C. Han, P. Zhao, S. Dib-Hajj, S. G. Waxman, Dynamic-clamp analysis of wild-type human  $Na_v1.7$  and erythromelalgia mutant channel L858H. *J. Neurophysiol.* **111**, 1429–1443 (2014).
21. S. D. Dib-Hajj, A. M. Rush, T. R. Cummins, F. M. Hisama, S. Novella, L. Tyrrell, L. Marshall, S. G. Waxman, Gain-of-function mutation in  $Na_v1.7$  in familial erythromelalgia induces bursting of sensory neurons. *Brain* **128**, 1847–1854 (2005).
22. C. Han, S. D. Dib-Hajj, Z. Lin, Y. Li, E. M. Eastman, L. Tyrrell, X. Cao, Y. Yang, S. G. Waxman, Early and late-onset inherited erythromelalgia: Genotype-phenotype correlation. *Brain* **132**, 1711–1722 (2009).
23. Y. Yang, S. D. Dib-Hajj, J. Zhang, Y. Zhang, L. Tyrrell, M. Estacion, S. G. Waxman, Structural modelling and mutant cycle analysis predict pharmacoresponsiveness of a  $Na_v1.7$  mutant channel. *Nat. Commun.* **3**, 1186 (2012).
24. K. Ørstavik, C. Weidner, R. Schmidt, M. Schmelz, H. Hilloges, E. Jørum, H. Handwerker, E. Torebjörk, Pathological C-fibres in patients with a chronic painful condition. *Brain* **126**, 567–578 (2003).
25. O. Uyanik, C. Quiles, H. Bostock, S. D. Dib-Hajj, T. Fischer, L. Tyrrell, S. G. Waxman, J. Serra, Spontaneous impulse generation in C-nociceptors of familial erythromelalgia (FE) patients. *Eur. J. Pain* **11**, S130–S293 (2007).
26. B. Namer, K. Ørstavik, R. Schmidt, I.-P. Kleggetveit, C. Weidner, C. Mørk, M. S. Kvernebo, K. Knut, H. Salter, T. H. Carr, M. Segerdahl, H. Quiding, S. G. Waxman, H. O. Handwerker, H. E. Torebjörk, E. Jørum, M. Schmelz, Specific changes in conduction velocity recovery cycles of single nociceptors in an erythromelalgia patient with the I848T gain-of-function mutation of  $Nav1.7$ . *Pain* **156**, 1637–1646 (2015).
27. J. J. Michiels, R. H. Te Morsche, J. B. Jansen, J. P. Drenth, Autosomal dominant erythromelalgia associated with a novel mutation in the voltage-gated sodium channel alpha subunit  $Nav1.7$ . *Arch. Neurol.* **62**, 1587–1590 (2005).
28. ClinicalTrials.gov [Internet]. Identifier: NCT02215252 A Clinical Trial To Evaluate PF-05089771 On Its Own And As An Add-On Therapy To Pregabalin (Lyrica) For The Treatment Of Pain Due To Diabetic Peripheral Neuropathy (DPN). Available from: <https://clinicaltrials.gov/ct2/show/NCT02215252>

**Acknowledgments:** We thank those subjects who participated in this study and their families. We thank F. Di Cesare for medical input into this study and S. Carolan and J. van Winkle for care of subjects and study management. We thank Z. Lin, D. Printzenhoff, M. Chapman, and N. Castle for PatchXpress characterization of PF-05089771 and PF-5153462. We thank H. Alexander and C. Campbell for help with figure design. We thank Roslin Cells Ltd. for generation of some of the iPSC lines used in this study. **Funding:** This study was funded by Pfizer Inc. The research leading to these results has received support from the Innovative Medicines Initiative Joint Undertaking under grant agreement no. 115439, resources of which are composed of financial contributions from the European Union's Seventh Framework Programme (FP7/2007–2013) and European Federation of Pharmaceutical Industries and Association (EFPIA) companies in kind contribution. M.M. was supported by an Industrial CASE Ph.D. studentship from the Biotechnology and Biological Sciences Research Council (BBSRC) in partnership with Pfizer. This publication reflects only the authors' views and neither the Innovative Medicines Initiative Joint Undertaking nor EFPIA nor the European Commission are liable for any use that may be made of the information contained therein. **Author contributions:** L.C., A.N., R.B., R.M.M., P.W., E.B.S., and J.B. designed the preclinical experiments. A.M. and Z.A. designed and executed the clinical study. L.C., A.A., P.-P.S., A.J.C.L., A.R.B., G.Y., and M.M. performed electrophysiological experiments. A.N. generated and differentiated iPSC lines, performed quality control, and carried out gene and protein expression. S.T. was the clinical study principal investigator. L.C., A.R., and M.M. analyzed electrophysiological data. A.N. and A.G. analyzed all iPSC and iPSC-SN-related molecular data. S.K. and P.S. provided statistical analyses of clinical and preclinical data. L.C., A.M., A.N., S.T., P.W., S.G.W., S.K., Z.A., J.B., and E.B.S. wrote the paper. **Competing interests:**  $Nav1.7$  sodium channel blockers described in this study are covered by patent WO/2010/079443; International Application No. PCT/IB2010/050033; publication date, 15 July 2010; International Filing Date, 06 January 2010. **Data and materials availability:** The ClinicalTrials.gov registration number for this study is NCT01769274 (28). Patient-derived iPSC lines are deposited in the European Bank for iPSCs (EBiSC; [www.ebisc.org/](http://www.ebisc.org/)) to whom initial enquiries for access should be addressed.

Submitted 29 October 2015

Accepted 1 April 2016

Published 20 April 2016

10.1126/scitranslmed.aad7653

**Citation:** L. Cao, A. McDonnell, A. Nitzsche, A. Alexandrou, P.-P. Saintot, A. J.C. Loucif, A. R. Brown, G. Young, M. Mis, A. Randall, S. G. Waxman, P. Stanley, S. Kirby, S. Tarabar, A. Gutteridge, R. Butt, R. M. McKernan, P. Whiting, Z. Ali, J. Bilsland, E. B. Stevens, Pharmacological reversal of a pain phenotype in iPSC-derived sensory neurons and patients with inherited erythromelalgia. *Sci. Transl. Med.* **8**, 335ra56 (2016).



## Pharmacological reversal of a pain phenotype in iPSC-derived sensory neurons and patients with inherited erythromelalgia

Lishuang Cao, Aoibhinn McDonnell, Anja Nitzsche, Aristos Alexandrou, Pierre-Philippe Saintot, Alexandre J.C. Loucif, Adam R. Brown, Gareth Young, Malgorzata Mis, Andrew Randall, Stephen G. Waxman, Philip Stanley, Simon Kirby, Sanela Tarabar, Alex Gutteridge, Richard Butt, Ruth M. McKernan, Paul Whiting, Zahid Ali, James Bilslan and Edward B. Stevens (April 20, 2016) *Science Translational Medicine* **8** (335), 335ra56. [doi: 10.1126/scitranslmed.aad7653]

### Editor's Summary

#### A gain in pain control

Subtype-specific blockade of sodium channel Nav1.7, which is important for firing of peripheral pain-signaling neurons, is a major focus of pain research. In a new study, Cao *et al.* created iPSC-derived sensory neurons from patients with inherited erythromelalgia (IEM), a painful disorder in which gain-of-function Nav1.7 mutations produce hyperexcitability and hyperresponsiveness to warmth in peripheral sensory neurons. The investigators show that a new selective Nav1.7 sodium channel blocker normalized the phenotype of iPSC-derived sensory neurons carrying IEM mutations and blocked pain perception in human subjects with IEM. These results provide proof of principle that selective Nav1.7 blockade may be useful in pain alleviation.

---

The following resources related to this article are available online at <http://stm.sciencemag.org>.  
This information is current as of April 20, 2016.

---

<b>Article Tools</b>	Visit the online version of this article to access the personalization and article tools: <a href="http://stm.sciencemag.org/content/8/335/335ra56">http://stm.sciencemag.org/content/8/335/335ra56</a>
<b>Supplemental Materials</b>	"Supplementary Materials" <a href="http://stm.sciencemag.org/content/suppl/2016/04/18/8.335.335ra56.DC1">http://stm.sciencemag.org/content/suppl/2016/04/18/8.335.335ra56.DC1</a>
<b>Permissions</b>	Obtain information about reproducing this article: <a href="http://www.sciencemag.org/about/permissions.dtl">http://www.sciencemag.org/about/permissions.dtl</a>

*Science Translational Medicine* (print ISSN 1946-6234; online ISSN 1946-6242) is published weekly, except the last week in December, by the American Association for the Advancement of Science, 1200 New York Avenue, NW, Washington, DC 20005. Copyright 2016 by the American Association for the Advancement of Science; all rights reserved. The title *Science Translational Medicine* is a registered trademark of AAAS.